



pISSN 2234-7518 • eISSN 2005-372X
<https://doi.org/10.4041/kjod24.260>
Korean J Orthod 2025;55(3):202-211

An effective approach to assessing inter-root distances using tooth models without repeated cone-beam computed tomography scans during orthodontic treatment

Haeun Moon^a 
Jaewon Koh^a 
Veerasathpurush
Allareddy^b 
Phimon Atsawasuwan^b 
Min Kyeong Lee^b 
Kyungmin Clara Lee^a 

^aDepartment of Orthodontics, School of Dentistry, Chonnam National University, Gwangju, Korea

^bDepartment of Orthodontics, College of Dentistry, University of Illinois Chicago, Chicago, IL, USA

Objective: To propose the utilization of virtual tooth models (VTMs) created by combining tooth root data from cone-beam computed tomography (CBCT) and crown data gathered through intraoral scanning to assess inter-root distance and angulation during orthodontic treatment when repeated radiographic monitoring becomes necessary. **Methods:** Patients with planned dental implant placement in edentulous areas during or after orthodontic treatment and who underwent intraoral and CBCT scans at the pretreatment and posttreatment stages were selected. Tooth models were fabricated by merging intraorally scanned crowns with the corresponding CBCT-scanned roots from the pretreatment. Tooth positions posttreatment was estimated by integrating models into posttreatment intraoral scans. Moreover, the actual positions were obtained from posttreatment CBCTs. Discrepancies in the estimated and actual tooth positions, including inter-radicular distances and inter-root angulations, were compared. **Results:** The minimum inter-radicular distance between two adjacent teeth demonstrated no significant difference between the estimated and actual tooth positions. The difference in inter-root angulation was not statistically significant. Most inter-radicular distances measured at each landmark revealed no significant differences between the estimated and actual tooth positions, except at the buccolingual midpoint of the cemento-enamel junction, where a slight discrepancy was observed. **Conclusions:** The tooth position of VTMs demonstrated clinically acceptable accuracy compared to CBCT scans. Additionally, VTMs can benefit both clinicians and patients by enabling accurate assessment of the inter-radicular space for dental implant placement without repeated CBCT scans.

Key words: Tooth model, Intraoral scans, Cone-beam computed tomography, Inter-radicular space

Received November 8, 2024; Revised January 28, 2025; Accepted March 10, 2025.

Corresponding author: Kyungmin Clara Lee.

Professor, Department of Orthodontics, School of Dentistry, Chonnam National University, 33 Yongbong-ro, Buk-gu, Gwangju 61186, Korea.

Tel +82-62-530-5864 e-mail ortholkm@jnu.ac.kr

Haeun Moon and Jaewon Koh contributed equally to this work.

How to cite this article: Moon H, Koh J, Allareddy V, Atsawasuwan P, Lee MK, Lee KC. An effective approach to assessing inter-root distances using tooth models without repeated cone-beam computed tomography scans during orthodontic treatment. Korean J Orthod 2025;55(3):202-211. <https://doi.org/10.4041/kjod24.260>

© 2025 The Korean Association of Orthodontists.

This is an Open Access article distributed under the terms of the Creative Commons Attribution Non-Commercial License (<http://creativecommons.org/licenses/by-nc/4.0>) which permits unrestricted non-commercial use, distribution, and reproduction in any medium, provided the original work is properly cited.

INTRODUCTION

Orthodontic treatment to open space for a missing tooth may be required to ensure adequate mesiodistal space for dental implant placement. During space opening, adjacent tooth crowns may tip apart, causing root convergence and reducing the space for implant placement. Therefore, orthodontic treatment must ensure that the adjacent tooth roots are parallel or slightly divergent.¹⁻⁴ Tipping of adjacent teeth can reduce the apical space and impact implant placement; therefore, a precise assessment of tooth movement during orthodontic treatment is essential. Although crown-level spaces can be easily evaluated, assessing root-level spaces remains challenging. Clinicians rely on radiographic images, including panoramic and periapical radiographs as well as cone-beam computed tomography (CBCT), as direct evaluation of the bone-level edentulous space is not feasible.

The concept of a three-dimensional (3D) virtual tooth model (VTM), which combines an intraorally scanned crown with a CBCT-scanned root, was introduced to balance two objectives: accurately evaluating the inter-radicular space and minimizing concerns about repeated radiographic exposure. By utilizing VTM, clinicians can monitor the root position at every stage by performing an intraoral scan of the occlusion and integrating it into the tooth model created during the pretreatment stage.^{5,6}

Previous studies have demonstrated that VTM can be applied to monitor root position during or after orthodontic treatment.⁷⁻⁹ Given the need for precise tolerance in dental implant placement, this study aimed to verify whether a VTM could be utilized to evaluate the edentulous space for implant placement. The objective of this study was to assess the accuracy of inter-radicular distance and inter-root angulation obtained from 3D VTM, combining intraorally scanned crowns and CBCT-scanned roots. Additionally, the study aimed to propose the use of the VTM for evaluating the edentulous space before implant placement.

MATERIALS AND METHODS

This retrospective study was approved by the Institutional Review Board of Chonnam National University, Gwangju, Korea (CNUHD-EXP-2019-018) and was conducted in compliance with the principles of the Declaration of Helsinki. The study included patients who underwent orthodontic treatment at Chonnam National University Dental Hospital, Gwangju, Korea. The requirement to obtain informed consent was waived.

The inclusion criteria were as follows: (1) missing teeth requiring dental implant placement during or after

orthodontic treatment and (2) patients with CBCT scans and intraoral-scanned data at the pretreatment and posttreatment stages. The exclusion criteria were as follows: (1) individuals with adjacent teeth defects requiring restorative treatment during orthodontics, (2) patients with incomplete or unavailable pretreatment and posttreatment records, (3) patients who had undergone interproximal reduction of adjacent teeth during treatment, and (4) those who had severe root resorption of adjacent teeth. This study was conducted in accordance with the guidelines of the Standards for Reporting of Observational Studies (STROBE) guidelines for cross-sectional studies.¹⁰

The sample size calculation was performed based on the results of a previous study by Park et al.,¹¹ which reported a mean difference of 1.42 ± 0.95 mm between simulated and actual inter-root distances. Using the formula for Cohen's *d* for paired samples, the effect size was derived and calculated as 1.49 through a priori power analysis in the G*Power program (version 3.1.9.2; Heinrich-Heine-University, Düsseldorf, Germany). With a statistical power of 90% and type 1 error rate of 5%, the calculation indicated that six cases were required to achieve adequate statistical power. Consequently, we selected six cases for each of the anterior and posterior implant areas (Table 1).

The concept and methodology of this study, utilizing the VTM are described in Figures 1 and 2, respectively. During the pretreatment and posttreatment stages, intraoral scans were obtained using a TRIOS 4 scanner (3Shape, Copenhagen, Denmark) and saved in the stereolithography (STL) format. The STL file was then exported to RapidForm software (3D Systems, Rockhill, SC, USA). After importing the pretreatment intraorally scanned data into the RapidForm software, the clinical crown areas of both adjacent teeth were selected following the gingival line. Using the inverse function, the

Table 1. Case description with implant placement areas used in this study

	Number
Anterior tooth implant area	
Maxillary central incisor	2
Maxillary lateral incisor	3
Maxillary canine	1
Posterior tooth implant area	
Maxillary first premolar	4
Mandibular second premolar	1
Mandibular first molar	1
Total	12

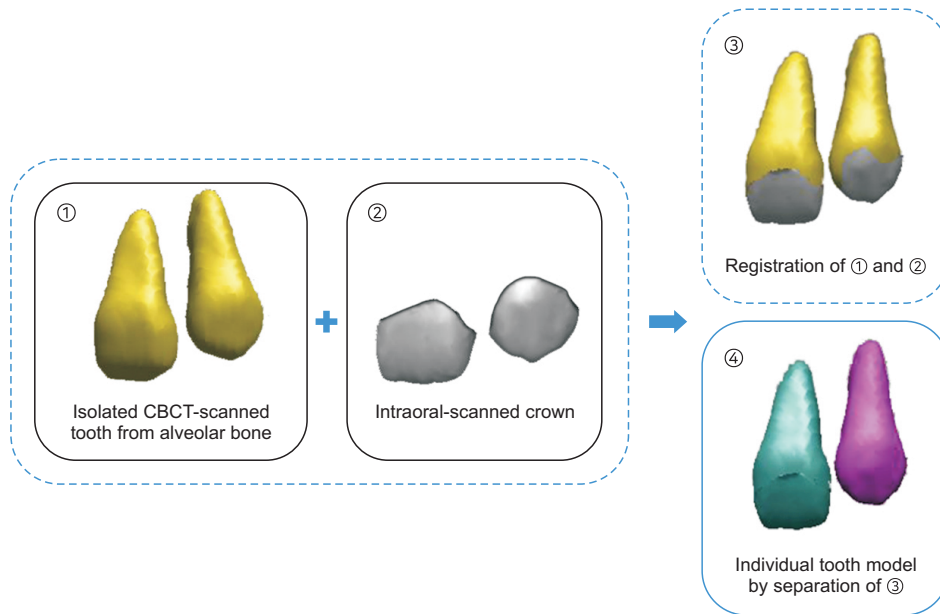


Figure 1. Fabrication of three-dimensional virtual tooth model (④). The isolated cone-beam computed tomography (CBCT)-scanned tooth from the alveolar bone (①) and intraoral-scanned crown (②) are registered and merged. The tooth model (③) is separated into individual tooth models.

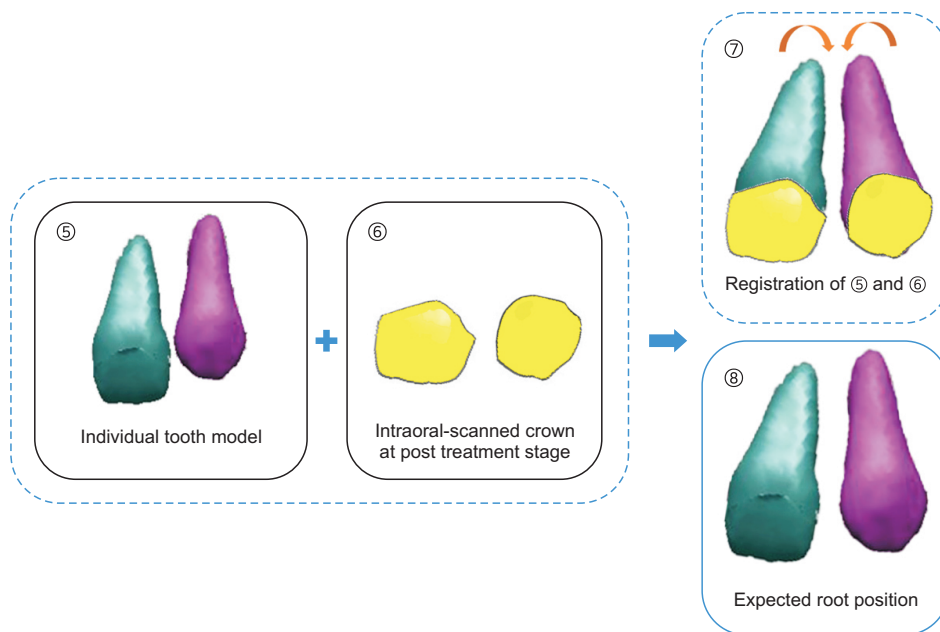


Figure 2. Estimation of root position using intraoral-scanned crown at the posttreatment stage and individual tooth models. After aligning the posttreatment model (⑤) with intraoral-scanned crown (⑥), the altered position (⑧) can be predicted in the direction indicated by the orange-colored arrows (⑦).

intraorally scanned data excluding the clinical crown areas were removed, leaving only two adjacent intraorally scanned crown images.

CBCT was performed using an Alphard Vega scanner

(Asahi Roentgen Co., Kyoto, Japan) set at a 200 × 179 mm field of view, 80 kV, 5 mA, and a voxel size of 0.39 mm. For 3D volume rendering and tooth segmentation, the CBCT data were imported into InViVo5 software

(version 5.1; Anatomage, San Jose, CA, USA). In the “medical design (MD)” tab in the software, each tooth was trimmed using the “sculpt” function, and mesh models were created. Considering that the threshold value setting (ISO value in this software) impacts the size of the segmented tooth models when creating the mesh models, an ISO value of 900 was employed for the crown and 600 for the root. Small ISO values result in clear imaging, enabling precise work. Intraorally scanned crown images and corresponding segmented tooth models made of CBCT-scanned data were imported into the Rapidform software. To minimize errors in the registration process, two CBCT tooth files—each representing an adjacent tooth—were individually imported, then merged using the “combine shell” function and registered as a pair. The registration process was performed following the same methodology as described in previous studies.^{5,6,9,11} By using the “Register” function in the program, segmented teeth from the CBCT scanned data and intraoral scanned crown were superimposed. “Initial registration” was performed by setting corresponding reference points both in the CBCT-tooth and intraoral-scanned crown images. These points included the left and right line angle points, the midpoint of the incisal edge, and the zenith. For the posterior teeth, points were selected from the cusp tips or fossa. For elaborate registration, “regional registration” was performed. The reference points for “regional registration” were the occlusal, buccal, and lingual surfaces of the crowns for the posterior teeth and the buccal, lingual, and incisal surfaces of the crowns for the anterior teeth. To create the VTM, which combined an intraorally scanned crown with a CBCT-scanned root, the crown portion of the CBCT tooth model was first removed. The VTM was then

generated by merging the intraoral-scanned crown with the crown-removed CBCT tooth model using the “combine shell” function (Figure 1).

To estimate the inter-radicular space for a dental implant without CBCT imaging and using only VTM at the pretreatment stage, we integrated the posttreatment intraoral scan (only crown data) and VTMs in the Rapidform software, utilizing the “initial registration” and “regional registration.” The tooth positions estimated from the VTMs were then compared with those measured using the posttreatment CBCT data (Figure 2). First, the 3D inter-radicular Euclidean distances between two adjacent teeth around the implant placement site were evaluated. As measurements of the Euclidean distances of the estimated tooth position in VTMs and the CBCT scan at the posttreatment stage required different software, setting reference points that could be picked identically in both software programs was crucial.

In this study, three reference planes and nine reference points were used (Figure 3). Ref 1 represents the plane connecting the most apical points of the cemento-enamel junction (CEJ) on both the buccal and lingual sides of each tooth. Ref 2 reference plane was defined as the midpoint between references 1 and 3. Ref 3 reference plane was established parallel to the Ref 1 reference plane, passing through the apical point of the shorter root of the two adjacent teeth. Reference points were designated as the midpoint of the buccal surface (1), proximal surface facing the edentulous site (2), and midpoint of the lingual surface (3) on each reference plane. The distances between these precise measurement points were then calculated. The midpoints of the labial, proximal, and lingual surfaces were defined as the most prominent points on each surface. Nine points were

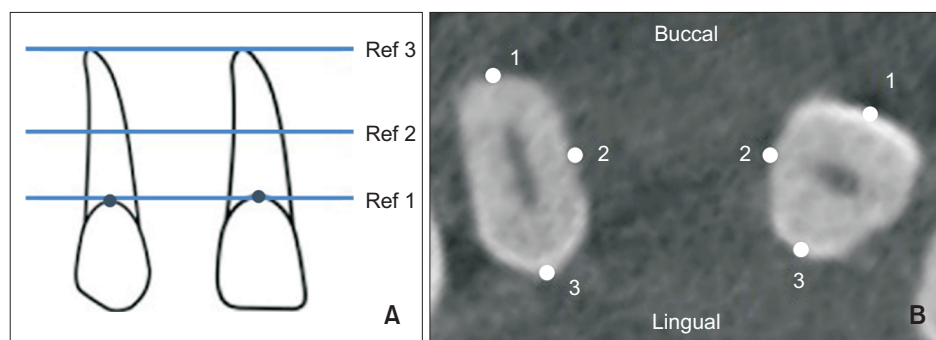


Figure 3. Reference planes (A) and reference points (B) used for linear measurements. Ref 1 represents the plane connecting the most apical points of the cemento-enamel junction on the buccal and lingual surfaces of the adjacent teeth to the edentulous area. Ref 2 is determined to be at the mid-level between Ref 1 and Ref 3. Ref 3 is established parallel to Ref 1, passing through the apical point of the shorter root of the two adjacent teeth. Reference points are designated as the midpoints of the buccal surface (1), proximal surface facing the edentulous site (2), and the midpoint of the lingual surface (3) on each reference plane. The distances between the same measurement points were calculated. A total of nine reference points were used, with three reference points assigned to each of the three planes.

measured for each tooth: CEJ1, CEJ2, CEJ3, mid-range 1 (MR1), MR2, MR3, apex 1 (AP1), AP2, and AP3 (Figure 3). The Euclidean inter-radicular distances were obtained from the distances between the corresponding points of two adjacent teeth. Measurement of the inter-radicular distances of the estimated tooth position via VTMs was performed using Rapidform software. By using the “parallel to plane” function, three reference planes were established. The distances were measured using the “point to point distances” function, with every corresponding point on each tooth being used for measurement. Assessment of the inter-radicular distances of the tooth position measured from the posttreatment CBCT was performed using the InViVo5 software. Before the measurement, the orientation was reset to obtain the same reference plane in the form of a cross-sectional image. Using the “reorientation” function in the software, orientation was adjusted in sagittal and coronal view to align the CEJ at the buccolingual midpoint of two adjacent teeth in the same plane. Considering the software provides a cross-sectional view, measurements between nine corresponding reference points were conducted using the “distance measurement” function.

Measurement of the minimum inter-radicular distances of the estimated tooth position was conducted

using the same methods applied for the inter-radicular distance measurements. Reference points for measurement were selected through visual inspection, typically at the most proximal and convex areas between the two teeth. Next, the inter-root angulation between two adjacent teeth at both the estimated and actual tooth positions was measured from the posttreatment CBCT using the “angle measurement function” in Rapidform and InViVo5 softwares, respectively (Figure 4).

All measurements were performed by a single investigator. The Shapiro–Wilk test was performed to confirm that the data followed a normal distribution, and a paired *t* test was conducted to compare the distance and angulation of the estimated values from the VTMs utilizing the tooth positions evaluated from the posttreatment CBCT. Differences were considered statistically significant at $P < 0.05$, and statistical analyses were performed using R Statistical software (version 2.14.0; R Foundation for Statistical Computing, Vienna, Austria). To compare the two measurements obtained from the estimated value using VTMs and the actual tooth position measured from the posttreatment CBCT graphically, the differences between the two methods were graphically plotted using Bland–Altman analysis (MedCalc Software Ltd., Ostend, Belgium). The significance level

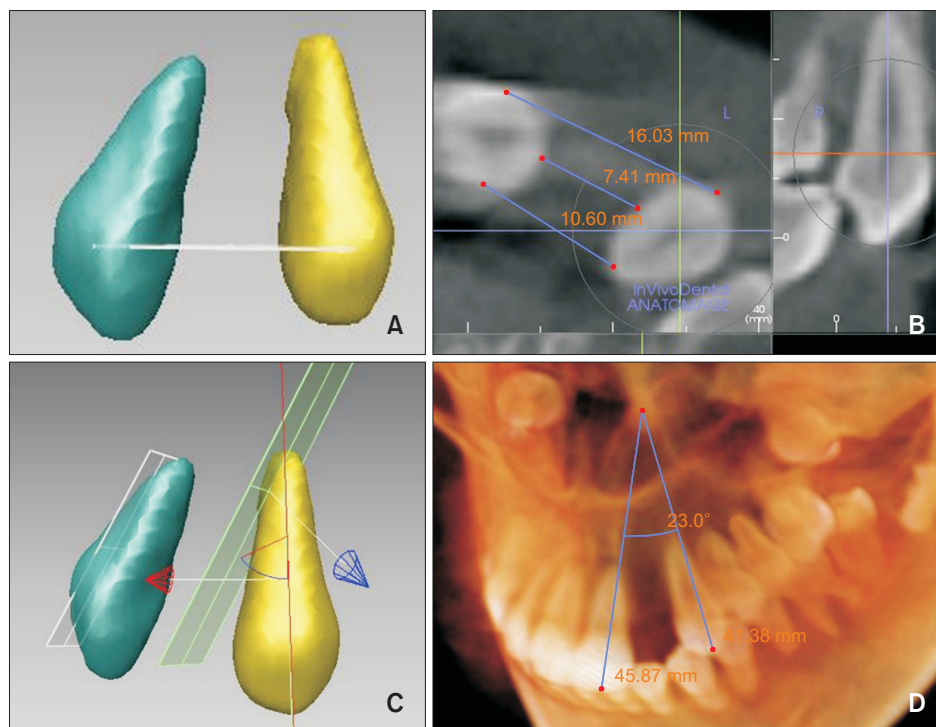


Figure 4. Linear and angular measurements in estimated and actual tooth position. **A**, Measurement of inter-radicular distance in estimated position using three-dimensional (3D) tooth model; **B**, Measurement of inter-radicular distance in actual position using cone-beam computed tomography (CBCT) image; **C**, Measurement of inter-root angulation in estimated position using 3D tooth model; **D**, Measurement of inter-root angulation in actual position using CBCT image.

was set at 5%.

To assess the study error, Dahlberg's formula was applied, with the same investigator performing measurements on 50% of the samples after a 14-day interval. Dahlberg's values demonstrated that the random error ranged from 0.15 to 0.38 mm. Additionally, the intra-class correlation coefficient (ICC) was used to assess the intraobserver repeatability. The ICC value of the repeated measurements indicated excellent agreement with a mean ICC of 0.97 (range, 0.95–0.99).

RESULTS

The means and standard deviations of the minimum inter-radicular distance difference between the tooth position estimated from the VTMs and that measured from posttreatment CBCT are demonstrated in Table 2. The minimum inter-radicular distance difference was -0.08 ± 0.88 mm in the anterior area, and -0.15 ± 0.21 mm in the posterior area, indicating that the estimated tooth position was underestimated. The total minimum inter-radicular distance difference was -0.11 ± 0.25 mm. The difference between the tooth position estimated from the VTMs and the position calculated from post-treatment CBCT was not statistically significant. For the inter-root angle, the mean difference and standard deviations were $0.33 \pm 1.26^\circ$ in the anterior area and $0.01 \pm 2.29^\circ$ in the posterior area. The total inter-root angle difference was $0.17 \pm 1.77^\circ$ (Table 3). Although no notable differences were observed between the tooth position estimated from the VTMs and that measured

from posttreatment CBCT, the discrepancy tended to be greater in the anterior area than in the posterior area. The means and standard deviations of the inter-radicular distances between the estimated and actual values at each level are listed in Table 4. All measurements except for CEJ1 and CEJ3 demonstrated minimal differences. In the anterior area, the measurements at the CEJ1 and CEJ3 levels were 0.41 ± 0.23 mm and 0.29 ± 0.21 mm, respectively. However, in the posterior area, the measurements at the CEJ3 level exhibited a difference of 0.30 ± 0.18 mm.

The accuracy of the method was visualized using Bland-Altman plots to investigate the validity of the estimated tooth positions. The horizontal axis represents the mean of the estimated and actual values, meanwhile, the vertical axis represents the difference between the estimated and actual values. A majority of the measurements were within the limit of agreement based on the Bland-Altman plots (Figure 5).

DISCUSSION

When teeth are lost, the adjacent teeth often drift into the edentulous space, making orthodontic treatment necessary for dental implant placement. Implant planning requires evaluation of three key dimensions: buccolingual, apicocoronal, and mesiodistal. The mesiodistal aspect is crucial for orthodontists, as treatment can modify the implant space by moving the adjacent teeth. This aspect is further divided into crown and root levels when planning implant placement. The proximity

Table 2. Comparison of minimum inter-radicular distance between the estimated and actual tooth positions

Minimum inter-radicular distance (mm)	Estimated tooth position	Actual tooth position	Difference	Significance (P value)
Anterior area	8.05 ± 1.69	8.14 ± 2.08	-0.08 ± 0.88	0.402
Posterior area	7.13 ± 2.34	7.28 ± 2.53	-0.15 ± 0.21	0.146
Total	7.59 ± 2.00	7.71 ± 2.25	-0.11 ± 0.25	0.053

Values are presented as mean \pm standard deviation.

The data represent the distance between the estimated and actual tooth positions at the minimum inter-radicular distance. Statistical significance was set at $P < 0.05$ using a paired *t* test.

Table 3. Comparison of inter-root angle between the estimated and actual tooth positions

Inter-root angle ($^\circ$)	Estimated tooth position	Actual tooth position	Difference	Significance (P value)
Anterior area	15.38 ± 5.22	15.05 ± 5.76	0.33 ± 1.26	0.549
Posterior area	20.13 ± 5.08	20.13 ± 3.81	0.01 ± 2.29	0.990
Total	17.75 ± 5.50	17.59 ± 5.35	0.17 ± 1.77	0.747

Values are presented as mean \pm standard deviation.

The data represent the inter-root angle between the estimated and actual tooth positions. Statistical significance was set at $P < 0.05$ using a paired *t* test.

Table 4. Comparison of inter-radicular distance between the estimated and actual tooth positions, measured at each level

Inter-radicular distance (mm)	Estimated tooth position	Actual tooth position	Difference	Significance (P value)
Anterior area				
CEJ1-CEJ1'	15.34 ± 1.17	14.93 ± 1.13	0.41 ± 0.23	0.007*
CEJ2-CEJ2'	8.47 ± 1.81	8.17 ± 1.92	0.31 ± 0.30	0.053
CEJ3-CEJ3'	12.50 ± 1.78	12.21 ± 1.70	0.29 ± 0.21	0.020*
MR1-MR1'	13.27 ± 1.57	13.21 ± 1.67	0.06 ± 0.53	0.794
MR2-MR2'	8.16 ± 1.80	8.01 ± 1.89	0.15 ± 0.59	0.567
MR3-MR3'	10.86 ± 2.23	10.78 ± 2.28	0.08 ± 0.13	0.182
AP1-AP1'	11.28 ± 1.19	11.20 ± 0.63	0.08 ± 0.66	0.771
AP2-AP2'	8.44 ± 1.49	8.44 ± 1.50	0.00 ± 0.07	> 0.999
AP3-AP3'	10.30 ± 1.32	10.32 ± 1.18	-0.02 ± 0.16	0.759
Posterior area				
CEJ1-CEJ1'	16.08 ± 2.41	15.79 ± 2.67	0.29 ± 0.63	0.309
CEJ2-CEJ2'	7.81 ± 1.89	7.66 ± 2.12	0.16 ± 0.63	0.571
CEJ3-CEJ3'	12.11 ± 3.19	11.82 ± 3.23	0.30 ± 0.18	0.011*
MR1-MR1'	14.08 ± 3.01	14.11 ± 3.15	-0.04 ± 0.39	0.821
MR2-MR2'	8.50 ± 4.18	8.41 ± 3.79	0.09 ± 0.49	0.658
MR3-MR3'	11.15 ± 3.95	10.91 ± 3.79	0.24 ± 0.26	0.074
AP1-AP1'	12.51 ± 6.41	12.57 ± 6.33	-0.06 ± 0.42	0.717
AP2-AP2'	9.45 ± 6.19	9.38 ± 6.25	0.06 ± 0.14	0.323
AP3-AP3'	11.06 ± 6.68	10.85 ± 6.59	0.21 ± 0.31	0.148

Values are presented as mean ± standard deviation.

The data represents the distance between the estimated and actual root positions at each level. The difference is obtained by subtracting the values of the actual root position from those of the estimated position. A negative value indicates an underestimation of the estimated distance.

CEJ, cemento-enamel junction; MR, mid-range; AP, apex.

*P < 0.05, paired t test.

See Figure 3 for definitions of each landmark or measurement.

of the adjacent teeth at the crown level is necessary to provide proximal support. Furthermore, the volume of the interdental papillae should also be evaluated. Ideally, the space for implant restoration should match that of the contralateral tooth.¹² The space at the crown level can be easily assessed either by directly measuring the width or using a dental cast. The preparation and evaluation of the root proximity of adjacent teeth is significantly challenging for clinicians as the space at the root level cannot be directly observed. Moreover, during the orthodontic space-opening process, adjacent teeth often tend to tip apart rather than moving parallel to one another. When the teeth tips are separated, the root tips converge, narrowing the space at the root level. Teeth with root proximity have very little interproximal bone, increasing the risk of lateral resorption and a decrease in vertical bone height.¹² As per recommendation, a

minimum of 1.0 mm of space between the implant and the adjacent root surface be secured to allow adequate healing and papilla development. If the space is too narrow, the use of a small-diameter implant should be considered.¹³ Constant communication between orthodontists and other specialists is essential to ensure that the required space is maintained.

Panoramic radiographs are commonly used to assess the inclination of the adjacent teeth and root proximity in the edentulous area. However, significant distortions, including enlargement and altered magnification, particularly in the canine and premolar regions, have been reported.¹⁴⁻¹⁶ In contrast, CBCT provides 3D imaging with minimal distortion, allowing for precise observation of root positions. However, concerns regarding radiation exposure make recommendation of repeated CBCT scans for patients difficult.

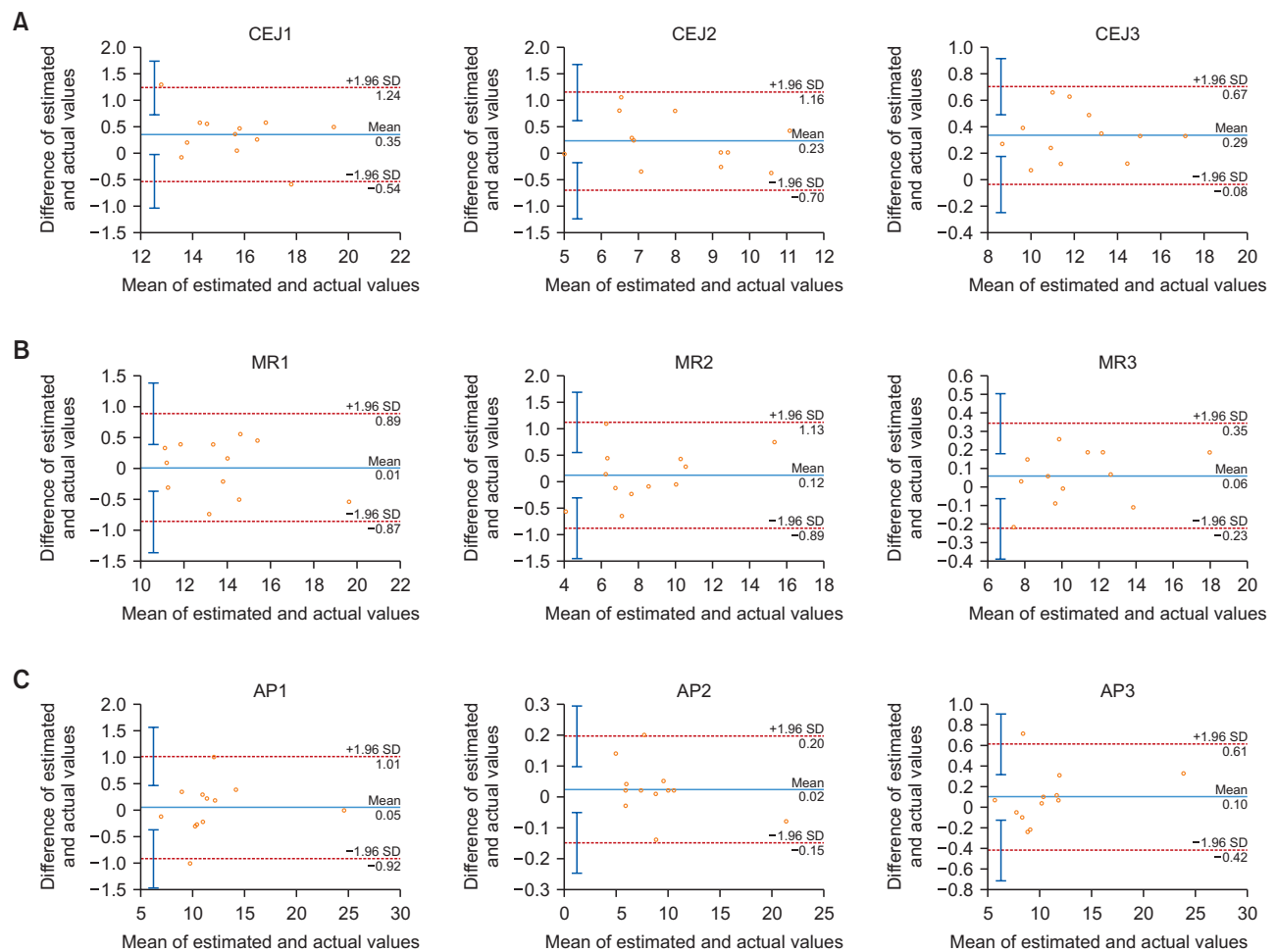


Figure 5. Bland–Altman plots for linear measurements (mm) in estimated and actual tooth positions. **A**, CEJ1, CEJ2, CEJ3; **B**, MR1, MR2, MR3; **C**, AP1, AP2, AP3.

CEJ, cemento-enamel junction; MR, mid-range; AP, apex; SD, standard deviation. See Figure 3 for definitions of each landmark or measurement.

The inter-radicular distance differences at the CEJ1 and CEJ3 levels were significant. The axial cross-sectional shape of the root varies at different levels, becoming wider and flatter mesiodistally at more coronal levels, which complicates the identification of the buccal and lingual midpoints. This likely contributed to the differences in the measurements between CEJ1 and CEJ3. This pattern remained consistent when analyzed according to the anterior and posterior teeth. In the anterior region, significant differences were observed between CEJ1 and CEJ3, whereas in the posterior region, only CEJ3 exhibited significant differences. Teeth with small superimposition areas, such as the upper lateral or lower central incisors, tend to demonstrate significant errors during superimposition.¹⁷ Posterior teeth provide various reliable reference points for superimposition, such as cusps, whereas anterior teeth rely on incisal edges

or buccolingual surfaces. Although the fabrication of VTMs was performed manually in this study, a technology to segment teeth using deep learning technology was recently proposed.^{9,18} Deep learning technology can significantly reduce the time and effort required by clinicians,⁹ while also enabling precise fabrication of VTMs with few potential errors. This advancement would not only benefit the fabrication process but also improve the dental implant planning process.¹⁹

CONCLUSIONS

The tooth position of VTMs demonstrated clinically acceptable accuracy compared to CBCT scans. Additionally, VTMs can benefit both clinicians and patients by enabling accurate assessment of the inter-radicular space for dental implant placement without repeated

CBCT scans. This study serves as a foundation for future research on evaluating root positions based solely on crown morphology.

AUTHOR CONTRIBUTIONS

Conceptualization: KCL. Data curation: HM, KCL. Formal analysis: HM, JK, KCL. Funding acquisition: KCL. Investigation: HM. Methodology: KCL, VA, PA, MKL. Project administration: KCL. Resources: KCL. Software: HM, JK, KCL. Supervision: KCL. Validation: KCL, VA, PA, MKL. Visualization: KCL. Writing—original draft: All authors. Writing—review & editing: All authors.

CONFLICTS OF INTEREST

No potential conflict of interest relevant to this article was reported.

FUNDING

This work was supported by the National Research Foundation of Korea (NRF) grant funded by the Korean government (Ministry of Science and ICT) (RS-2025-00516911).

SUPPLEMENTARY VIDEO

A video presentation of this article is available at <https://youtu.be/BkpxGND67IQ>

REFERENCES

- Richardson G, Russell KA. Congenitally missing maxillary lateral incisors and orthodontic treatment considerations for the single-tooth implant. *J Can Dent Assoc* 2001;67:25-8. <https://pubmed.ncbi.nlm.nih.gov/11209502/>
- Sabri R. Management of missing maxillary lateral incisors. *J Am Dent Assoc* 1999;130:80-4. <https://doi.org/10.14219/jada.archive.1999.0032>
- Kokich V. Early management of congenitally missing teeth. *Semin Orthod* 2005;11:146-51. <https://doi.org/https://doi.org/10.1053/j.sodo.2005.04.008>
- Olsen TM, Kokich VG Sr. Postorthodontic root approximation after opening space for maxillary lateral incisor implants. *Am J Orthod Dentofacial Orthop* 2010;137:158.e1; discussion 158-9. <https://doi.org/10.1016/j.ajodo.2009.08.024>
- Lee K, Lee GH. Application of 3D tooth model for monitoring of implant space and inter-root distance without radiographs: a proof of concept study. *Int J Implant Dent* 2020;6:55. <https://doi.org/10.1186/s40729-020-00253-3>
- Lee KM. Application of individual composite tooth model for monitoring of tooth movement during orthodontic treatment. *Clin J Korean Assoc Orthod* 2020;10:228-37. <https://doi.org/10.33777/cjkao.2020.10.3.228>
- Lee RJ, Pi S, Park J, Devgon D, Nelson G, Hatcher D, et al. Accuracy and reliability of the expected root position setup methodology to evaluate root position during orthodontic treatment. *Am J Orthod Dentofacial Orthop* 2018;154:583-95. <https://doi.org/10.1016/j.ajodo.2018.05.010>
- Lee RJ, Ko J, Park J, Pi S, Devgon D, Nelson G, et al. Accuracy and reliability of the expected root position setup on clinical decision making of root position at midtreatment. *Am J Orthod Dentofacial Orthop* 2019;156:566-73. <https://doi.org/10.1016/j.ajodo.2019.03.018>
- Lee SC, Hwang HS, Lee KC. Accuracy of deep learning-based integrated tooth models by merging intraoral scans and CBCT scans for 3D evaluation of root position during orthodontic treatment. *Prog Orthod* 2022;23:15. <https://doi.org/10.1186/s40510-022-00410-x>
- von Elm E, Altman DG, Egger M, Pocock SJ, Gøtzsche PC, Vandenbroucke JP. The Strengthening the Reporting of Observational Studies in Epidemiology (STROBE) statement: guidelines for reporting observational studies. *J Clin Epidemiol* 2008;61:344-9. <https://doi.org/10.1016/j.jclinepi.2007.11.008>
- Park M, Allareddy V, Atsawasuwan P, Lee MK, Lee KC. Consideration of root position in virtual tooth setup for extraction treatment: a comparative study of simulated and actual treatment results. *Korean J Orthod* 2023;53:26-34. <https://doi.org/10.4041/kjod22.105>
- Jivraj S, Reshad M. Esthetic implant dentistry: diagnosis and treatment planning. In: Fonseca RJ, ed. *Oral and maxillofacial surgery*. 3rd ed. St. Louis: Elsevier; 2018. p. 391-409. <https://www.clinicalkey.es/#!/content/book/3-s2.0-B9780323414999000261>
- Rose TP, Jivraj S, Chee W. The role of orthodontics in implant dentistry. *Br Dent J* 2006;201:753-64. <https://doi.org/10.1038/sj.bdj.4814349>
- Samawi SS, Burke PH. Angular distortion in the orthopantomogram. *Br J Orthod* 1984;11:100-7. <https://doi.org/10.1179/bjo.11.2.100>
- Peck JL, Sameshima GT, Miller A, Worth P, Hatcher DC. Mesiodistal root angulation using panoramic and cone beam CT. *Angle Orthod* 2007;77:206-13. [https://doi.org/10.2319/0003-3219\(2007\)077\[0206:Mraupa\]2.0.Co;2](https://doi.org/10.2319/0003-3219(2007)077[0206:Mraupa]2.0.Co;2)
- Owens AM, Johal A. Near-end of treatment panoramic radiograph in the assessment of mesiodistal root angulation. *Angle Orthod* 2008;78:475-81.

- <https://doi.org/10.2319/040107-161.1>
17. Sun L, Hwang HS, Lee KM. Registration area and accuracy when integrating laser-scanned and maxillofacial cone-beam computed tomography images. *Am J Orthod Dentofacial Orthop* 2018;153:355-61. <https://doi.org/10.1016/j.ajodo.2017.06.027>
 18. Ayidh Alqahtani K, Jacobs R, Smolders A, Van Gerwen A, Willems H, Shujaat S, et al. Deep convolutional neural network-based automated segmentation and classification of teeth with orthodontic brackets on cone-beam computed-tomographic images: a validation study. *Eur J Orthod* 2023;45:169-74. <https://doi.org/10.1093/ejo/cjac047>
 19. Bianchi J, Mendonca G, Gillot M, Oh H, Park J, Turkestani NA, et al. Three-dimensional digital applications for implant space planning in orthodontics: a narrative review. *J World Fed Orthod* 2022;11:207-15. <https://doi.org/10.1016/j.ejwf.2022.10.006>